# Measurement of higher order chromatic dispersion in a photonic bandgap fiber: comparative study of spectral interferometric methods

T. Grósz,[1,*] A. P. Kovács,[1] M. Kiss,[1] and R. Szipőcs[2]

[1]Department of Optics and Quantum Electronics, University of Szeged, Dóm tér 9, H-6720 Szeged, Hungary

[2]Institute for Solid State Physics and Optics, Wigner RCP, Konkoly Thege út 29-33, H-1121 Budapest, Hungary

*Corresponding author: tgrosz@titan.physx.u-szeged.hu

Received 26 November 2013; revised 7 February 2014; accepted 13 February 2014; posted 14 February 2014 (Doc. ID 201474); published 19 March 2014

Chromatic dispersion of a 37 cm long, solid-core photonic bandgap (PBG) fiber was studied in the wavelength range of 740–840 nm with spectral interferometry employing a Mach–Zehnder interferometer and a high resolution spectrometer. The interferometer was illuminated by a Ti:sapphire laser providing 20 fs pulses. A comparative study has been carried out to find the most accurate spectral phase retrieval method that is suitable for measuring higher order chromatic dispersion. The stationary phase point, the minima–maxima, the cosine function fit, the Fourier transform, and the windowed Fourier transform methods were tested. It was shown that out of these five techniques, the Fourier-transform method provided the dispersion coefficients with the highest accuracy, and it could also detect rapid phase changes in the vicinity of leaking mode frequencies within the transmission band of the PBG fiber. 

*OCIS codes:* (060.2300) Fiber measurements; (060.4005) Microstructured fibers; (120.3180) Interferometry.

http://dx.doi.org/10.1364/AO.53.001929

## 1. Introduction

Nowadays, there are numerous applications of optical fibers, and the demand for further development is continuously growing. The attempt to extend the current limits of performance drew interest toward new alternatives. By moving away from constraints of conventional fiber optics, Bragg-type [1,2] and photonic crystal fibers [3–10] have created new opportunities and acquired respectable attention due to their unique dispersion, birefringent, nonlinear, and guiding characteristics, which can be tailored by the proper design of their geometrical structure.

As one enticing feature of photonic crystal fibers is the feasibility of dispersion-free propagation, a lot of effort is made to develop appropriate geometries that satisfy such requirements [3–5,7–10]. For instance, nearly zero dispersion over a large bandwidth can be realized in hollow-core, air-silica photonic bandgap (PBG) fibers or solid-core Bragg fibers with step-index profile by introducing resonant structures in the fiber cladding [10]. These fiber constructions might have interesting applications in nonlinear wavelength conversion systems or fiber delivery systems for femtosecond pulses. According to the uncertainties in modeling and manufacturing, for practical fiber laser systems it is necessary to characterize the chromatic dispersion of the realized fiber samples as accurately as possible in assistance to their further development or quality testing.

There are several dispersion measurement methods, such as the time of flight, the modulation phase shift, and the interferometric technique [11,12]. The former two methods require long lengths of fiber, which is not a desirable feature if specialty fibers

1559-128X/14/091929-09$15.00/0

under development are examined [12]. Interferometric techniques, however, are not only capable of measuring dispersion of shorter fibers but are more precise than the previous ones. There are two types of interferometric methods: temporal and spectral. Spectral interferometry is generally more stable than the temporal version and reliable if higher order dispersion is of concern [12]. It is a commonly used technique to measure the spectral phase and the amplitude spectrum. The recorded interferograms can be evaluated with different techniques. One of the most common evaluation methods is the stationary phase point (SPP) method [13], which is often used for dispersion characterization of optical elements but also applicable for fibers [14–16]. Another method is the minima–maxima (MM) [15,17–20], which has been already used to measure the dispersion of photonic crystal fibers by Jasapara *et al.*[17] The so-called cosine function fit (CFF) method [21,22], which relies on fitting a phase modulated cosine function to the normalized interferogram, has also been successfully used to measure the dispersion and refractive index of microstructured [21] and photonic crystal fibers [22]. Another alternative is the Fourier-transform (FT) method [23–30], which is a widely used technique for determining the dispersion of mirrors and glass slabs [24,25] but also finds its application in measuring the spectral phase of microstructured [27] and dispersion compensating fibers [29]. Recently, the windowed Fourier-transform (WFT) [28,30–33], which is commonly used in surface profilometry [28,30], has been also applied in order to retrieve the spectral phase of a beam splitter [31] and mirrors [32,33].

Describing the dispersion of a fiber in a form of coefficients of the Taylor expansion of the spectral phase is a common practice [14,18,21,24,27]. Usually, the dispersion resulting from propagation in glasses or fibers is determined up to the third order [14,18,21,24], although there have been proposals up to the sixth-order dispersion retrieval [27]. In the case of tailored PBG fibers with reduced second order dispersion, the effect of the higher order dispersion terms on the pulse propagation may become significant [9]. Thus, it would be of great advantage to find the most precise evaluation method for phase retrieval that is sensitive to higher order dispersion. It would be significantly important to find a method that could provide precise information on how the presence of leaking modes, which might appear within the bandgap of these fibers [6], affects the accuracy of the measurements. In order to resolve such irregularities in the confinement loss spectrum, which result in phase jumps in the spectral phase, high resolution measurement is a basic requirement.

There are three possibilities to test the precision of the evaluation methods, one of which is theoretical analysis. The influence of the calibration of the detector on spectral interferometry [25] and the experimental noise in the case of the FT method [26] has already been investigated. Because of the number of factors that need to be taken into account, such analyses are rather complex. Another way is to use simulations to study the effects of a few factors, as was done in the case of the FT and WFT methods in profilometry [30]. A study to find the optimal parameters for the WFT method has also been presented [31]. Börzsönyi *et al.* have also studied the influence of some parameters, such as noise, computation error, and visibility in the case of a CFF-like method in spectrally and spatially resolved interferometry [34]. Yet another possibility is comparing methods by measuring fiber samples in which case various error sources are present and their collective effects can be well investigated.

In this paper, we present a comparative study of the five mentioned spectral interferometric methods in measuring a short-length fiber on the spectral range of 740–840 nm, regarding accuracy and sensitivity to higher order dispersion. The sample is a Bragg-type solid-core PBG fiber having a quasi-periodic refractive index versus radius profile with cylindrical symmetry. Whereas it would be beneficial to compare the evaluation methods by theoretical analyses and simulations as well, this is beyond the scope of the paper.

## 2. Theory

Spectral interferometry is a widely used technique for precise dispersion measurement of optical elements, such as fibers. The basic concept of the technique is utilizing a two-beam interferometer, usually a Michelson or a Mach–Zehnder type. For illumination, a broadband light source, for example a tungsten halogen lamp, a light emitting diode, amplified spontaneous emission, a super continuum source, or ultrashort laser pulses, can be used. The optical element under study is placed in one, the so-called sample arm of the interferometer. By adjusting the length of the other, the reference arm, at certain time delays $\tau$ between the two arms interference fringes can be observed at the output of a spectrometer or spectrograph placed behind the interferomter. The frequency-dependent intensity distribution $I(\omega)$ of the interferogram at the output of the spectrometer can be described as

$$I(\omega) = I_r(\omega) + I_s(\omega) + 2\sqrt{I_r(\omega) \cdot I_s(\omega)} \cdot \cos(\Phi(\omega)), \tag{1}$$

where $I_r$ and $I_s$ are the spectral intensity of the reference and the sample arms, respectively. $\Phi$ is the spectral phase difference between the arms:

$$\Phi(\omega) = \varphi(\omega) + \omega\tau, \tag{2}$$

where $\varphi(\omega)$ is the spectral phase function of the sample and $\tau$ is the time delay between the pulses from the two arms calculated from their geometrical path length difference measured in air.

When an ultrashort laser pulse is traveling through a dispersive optical element, e.g., a fiber, its temporal profile undergoes a change. If the variation

in the amplitude of the spectral components of the pulse can be neglected, the change in the temporal profile is only determined by the spectral phase $\varphi(\omega)$ of the fiber. To characterize the spectral phase function, usually the Taylor-expansion of the $\varphi(\omega)$ is taken around the carrier frequency $\omega_0$ of the pulse:

$$\varphi(\omega) = \varphi(\omega_0) + \mathrm{GD}(\omega-\omega_0) + \frac{\mathrm{GDD}}{2}(\omega-\omega_0)^2 + \frac{\mathrm{TOD}}{6}(\omega-\omega_0)^3 + \frac{\mathrm{FOD}}{24}(\omega-\omega_0)^4 + \frac{\mathrm{QOD}}{120}(\omega-\omega_0)^5 + \ldots, \quad (3)$$

where

$$\mathrm{GD} = \left.\frac{d\varphi}{d\omega}\right|_{\omega=\omega_0}, \qquad \mathrm{GDD} = \left.\frac{d^2\varphi}{d\omega^2}\right|_{\omega=\omega_0},$$
$$\mathrm{TOD} = \left.\frac{d^3\varphi}{d\omega^3}\right|_{\omega=\omega_0},$$
$$\mathrm{FOD} = \left.\frac{d^4\varphi}{d\omega^4}\right|_{\omega=\omega_0}, \qquad \mathrm{QOD} = \left.\frac{d^5\varphi}{d\omega^5}\right|_{\omega=\omega_0} \quad (4)$$

are the derivatives of the spectral phase with respect to angular frequency. The dispersion coefficients are called the group delay (GD), the group delay dispersion (GDD), and the third- (TOD), fourth- (FOD) and fifth-order dispersion (QOD), respectively. As specific pulse distortions can be connected to these coefficients, and in practice it is useful if the dispersion of an optical element can be described by some coefficients, often not only the spectral phase curve is measured, but these coefficients are also determined by fitting a polynomial to the curve.

In the case of photonic crystal or bandgap fibers, it may occur that their spectral phase function cannot be approximated well with a Taylor-series on certain spectral ranges (e.g., in the vicinity of leaking modes). In these cases only the experimental methods can be used for the precise characterization of the dispersion, which are based on the direct measurement of the spectral phase function.

In the case of the CFF evaluation method, to have the phase as the function of the frequency, the following normalization should be performed on the spectral interferogram [22]:

$$\cos(\Phi(\omega)) = \frac{I(\omega) - I_r(\omega) - I_s(\omega)}{2\sqrt{I_r(\omega)\cdot I_s(\omega)}}, \quad (5)$$

as the fit of the cosine function requires interferograms with constant amplitudes. This normalization is also useful for the SPP and the MM methods as the shift of the intensity peaks caused by the nonconstant spectrum is canceled and the precision of these methods become higher. However, the FT methods do not require this normalization.

By examining the conditions of formation of the extreme values

$$\frac{d(\cos(\Phi(\omega)))}{d\omega} = -\sin(\Phi(\omega))\cdot\frac{d\Phi}{d\omega} = 0, \quad (6)$$

we get two evaluation methods that will be discussed in the following.

### A. Stationary Phase Point Method

Consider first the case when Eq. (6) is fulfilled by the condition $d\Phi/d\omega = 0$. At the frequency where this condition is true, a so-called stationary phase point is formed, around which the phase changes very slowly. The position of the SPP in the interferogram changes if the delay of the reference arm is adjusted because the condition of forming a stationary phase point is then fulfilled at another frequency. By rearranging Eq. (2) at the SPP we get

$$\frac{d\varphi}{d\omega} = -\tau. \quad (7)$$

Note that if the spectral phase $\varphi$ is a third-order curve, Eq. (7) has two solutions, which means that two SPPs are formed. In that case, both SPPs should be monitored.

By examining the positions of the SPPs at different arm lengths, the sign and the magnitude of the GD can be retrieved [13–16], as it can be seen from Eq. (7). By plotting the group delay as a function of the frequency and fitting a polynomial of appropriate order to the curve, the dispersion coefficients can be retrieved:

$$\mathrm{GD}_{\mathrm{fit}} = a_0 + a_1\Delta\omega + a_2\Delta\omega^2 + a_3\Delta\omega^3 + a_4\Delta\omega^4, \quad (8)$$

where $a_0, a_1, \ldots$ denote the fitting coefficients and $\Delta\omega = \omega - \omega_0$. The fitting parameters in the function above correspond to the coefficients of the Taylor-expansion of the spectral phase in Eq. (3), i.e., $\mathrm{GD} = a_0$, $\mathrm{GDD} = a_1$, $\mathrm{TOD} = 2a_2$, $\mathrm{FOD} = 6a_3$, and $\mathrm{QOD} = 24a_4$. Note that if, for instance, a polynomial of the fourth order is fitted to the GD curve, the dispersion coefficients are retrieved up to the fifth order.

In the case of optical fibers, the dispersion values might be quite high; thus at some parts of the interferogram the fringes become too dense to be resolved by the spectrometer. In such cases dispersion retrieval with the SPP method is a reliable possibility. One drawback of the method is that for a precise measurement it requires reading a lot of interferograms one by one, which is time-consuming. In the case of lower dispersion, the SPP spreads and the method becomes inaccurate.

### B. Minima–Maxima Method

Another evaluation method can be used when Eq. (6) is fulfilled by the other condition. The $\sin(\Phi(\omega)) = 0$ condition gives the positions of the intensity minima

and maxima [15,17–20]. The extreme points are formed at the frequencies where the phase $\Phi$ is equal to $\pi$ times a whole number. First of all, the recorded interferogram is normalized and then the relative angular frequencies belonging to the intensity minima and maxima are determined. To assign the phase with the extreme points, the order number $(m)$ corresponding to a minimum or maximum is multiplied by $\pi$. If the resulting phase values are plotted as a function of the relative angular frequency and a polynomial is fitted to the data, the fitting coefficients give the values of the dispersion coefficients:

$$\Phi_{\text{fit}} = b_0 + b_1\Delta\omega + b_2\Delta\omega^2 + b_3\Delta\omega^3 + b_4\Delta\omega^4 + b_5\Delta\omega^5, \quad (9)$$

where $b_0, b_1, \ldots$ correspond to the coefficients of the Taylor-expansion of the spectral phase. By fitting a polynomial of the fifth order to the phase curve, the dispersion coefficients are retrieved up to the fifth order: $\text{GD} = b_1$, $\text{GDD} = 2b_2$, $\text{TOD} = 6b_3$, $\text{FOD} = 6b_4$, and $\text{QOD} = 24b_5$.

The advantage of the MM method is its insensitivity to noise and the sufficiency of one interferogram along with the reference and sample arm spectra. As the cosine function is odd function, there is an ambiguity in the sign of the dispersion coefficients. Evaluating another interferogram belonging to another time delay, the signs can be determined.

### C. Phase Modulated Cosine Function Fit Method

The main advantage of this evaluation compared to the previously introduced methods is that it is quick and requires only one interferogram along with the reference and sample arm spectrum to provide information about the spectral phase of the optical element under study. When the normalized spectral interferogram is generated according to Eq. (5), an appropriate order of phase-modulated cosine function can be fitted: [21,22]

$$I_{\text{fit}} = c_1 + c_2\cos(b_0 + b_1\Delta\omega + b_2\Delta\omega^2 + b_3\Delta\omega^3 + b_4\Delta\omega^4 + b_5\Delta\omega^5), \quad (10)$$

where $b_0, b_1, \ldots$ have the same meaning as in the case of the MM method and $c_1$ and $c_2$ are fitting parameters.

One drawback of the method comes to light when large dispersion values are measured, which causes the fringes to become too dense. Since the visibility of the interference fringes start decreasing due to the finite resolving power of the spectrometer, the determined dispersion coefficients and thus the calculated spectral phase become inaccurate.

### D. Fourier-Transform Method

The next method we consider is the FT method [23–30]. This method requires a dense interference pattern that is achievable by setting a relatively large, at least a couple of picoseconds delay between the reference and sample signals. First a Fourier transform is performed on an interferogram given by Eq. (1):

$$F\{I(\omega)\} = F\{I_r(\omega)\} + F\{I_s(\omega)\} + F\left\{2\sqrt{I_r(\omega)\cdot I_s(\omega)}\cdot\cos(\Phi(\omega))\right\}. \quad (11)$$

The resulting function $I(t)$ in the time domain is

$$I(t) = I_r(t) + I_s(t) + I_i(t-\tau') + I_i(t+\tau'), \quad (12)$$

where $I(t)$, $I_r(t)$ and $I_s(t)$ are the FT pairs of $I(\omega)$, $I_r(\omega)$, and $I_s(\omega)$. Note that it is not the time profile of the signals. $I_i(t-\tau')$ and $I_i(t+\tau')$ are the so-called interference terms at the time delays $\tau$ and $-\tau$.

In the next step of the evaluation, the peak at the positive delay $I_i(t-\tau')$ is filtered. By taking the inverse FT of this signal, the spectral phase is retrieved. By fitting a polynomial to the measured phase curve, the dispersion coefficients can be determined.

The main advantage of the method is that it can be well automatized, also requires only one interferogram, and allows a direct measurement of the spectral phase.

### E. Windowed Fourier-Transform Method

Another evaluation, also based on the FT, is the so-called windowed FT method [28,30–33]. During the evaluation, the measured spectral interferogram is multiplied by a window function, in general a Gaussian function:

$$I_w(\omega,\Omega) = I(\omega)\exp\left[-\left(\frac{\omega-\Omega}{\Delta\Omega}\right)^2\right]. \quad (13)$$

The width $\Delta\Omega$ of the window function is much smaller than that of the spectrum of the pulse. If the central frequency $\Omega$ of the window function is changed, we get a series of the windowed interferograms as a result. When a FT is applied on the windowed interferograms, a similar signal is obtained as in Eq. (12), but in this case the time delay $\tau'$ of the interference term is frequency dependent. Determining the time delays belonging to the peaks of the interference terms, the group delay is retrieved as a function of the frequency. As in the previous methods, a polynomial fitting to this curve gives the dispersion coefficients. An important issue is how to choose the values of the $\Omega$ and $\Delta\Omega$ [31].

## 3. Experimental Setup

The experimental setup can be seen in Fig. 1. It consisted of a combination of a Mach–Zehnder interferometer and a high resolution spectrometer (Ocean Optics, HR4000). The spectral range of the spectrometer was 700–900 nm with a resolution of 0.1 nm. As a broadband light source, a Ti:sapphire oscillator

(20 fs at 800 nm, FWHM = 60 nm) was used. The fiber under study was a 37 cm long, large mode area (LMA) solid-core PBG fiber similar to that described in detail by Fevrier *et al.* in [35]. The preform of our sample was prepared by a MCVD process. According to refractive index profile measurements on the preform, it has an aperiodic Bragg fiber structure exhibiting circular, alternating high and low index regions around the core that has the same refractive index as that of the low index layers. The low index layers are made of fused silica, while the refractive indices of the high index layers are higher by ~0.0125 approximately due to Ge doping. Because of evaporation/diffusion of the Ge dopant during the manufacturing process, however, the measured refractive index transitions are very smooth. The estimated core radius of the fiber is $R_c \sim 8$ μm. The number of HL periods in the cladding region is eight. Starting from the core, physical thickness values of the high and low index layers gradually increases by approximately 50%, which results in a bandgap centered at around 810 nm and some leaking modes at 783 and 813 nm. Because of the effect of anomalous waveguide dispersion, our PBG fiber sample has considerably lower dispersion than a conventional single mode silica fiber. The laser pulses were launched into the fiber by a microscope objective (NA = 0.5, 25×), and the output pulses were collimated by a lens of 18 mm focal length. The area marked with dashed lines denotes the adjustable part of the reference arm. A filter was inserted in the reference arm to equalize the intensity of the reference and sample beams. As the fiber had a slight birefringence, a polarizer was placed in front of the spectrometer to improve the visibility.

## 4. Results and Discussion

In this section, the results produced by the previously introduced five evaluation methods are presented. 60 interferograms were recorded at different delays of the reference arm. In some of the recorded normalized interferograms, two SPPs appeared in the evaluation range (see Fig. 2). As shown previously [36] the presence of two SPPs suggests significant third-order dispersion. As implied earlier, contrary to conventional optical fibers, the higher order dispersion terms in the spectral phase may also have a significant role in the case of PBG fibers; thus in the first approach the coefficients were determined up to the fourth order.

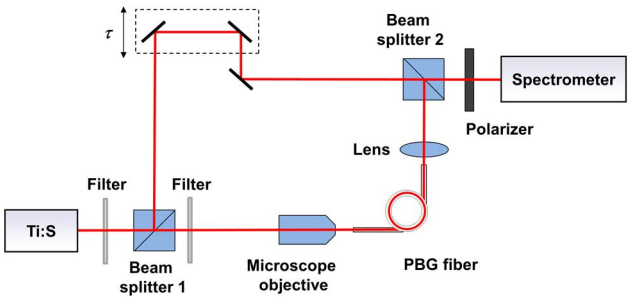


Fig. 1. Experimental setup.

First, the SPP method was used to measure the group delay caused by the PBG fiber. The positions of the SPPs were determined using 24 interferograms in which the SPPs appeared, i.e., from −1600 to 0 fs relative delays between the sample and the reference pulse. Note that the negative relative delay means that the reference arm is the longer one. In order to retrieve the dispersion coefficients up to the fourth order a third-order polynomial was fitted to the measured group delay curve. The difference between the fitted and the measured curve is quite significant, as can be seen in Fig. 3(a). In order to improve the precision, a fourth-order polynomial was also fitted and the coefficients were determined up to the fifth order. In this case the difference between the measured and the fitted curve is smaller [Fig. 3(b)], denoting the presence of fifth-order dispersion. By examining the spectrum of the sample arm, resonances can be seen at 783 and 813 nm. The fiber has a sharp cut-off at 838 nm, which shortened the evaluation range given by the otherwise broader spectrum of the Ti:S laser [Fig. 3(c)]. Unfortunately, although the movement of the SPP changes in the vicinity of the resonances of the fiber, the poor wavelength resolution does not allow measuring the peaks in the spectral phase in this region.

As the fourth-order fit seems to be more accurate than the third, only the retrieved group delay and the fourth-order fitted polynomial are displayed in Fig. 4. Despite the smaller misfit achieved by fitting a polynomial of the fourth order, we have concluded that this method does not provide any information regarding the accuracy of the evaluation in the regions of the leaking mode frequencies.

The dispersion coefficients were also measured by determining the positions of intensity minima and maxima on 30 normalized spectral interferograms. The range of the evaluation was a bit wider as the presence of the SPP was not a requirement; thus

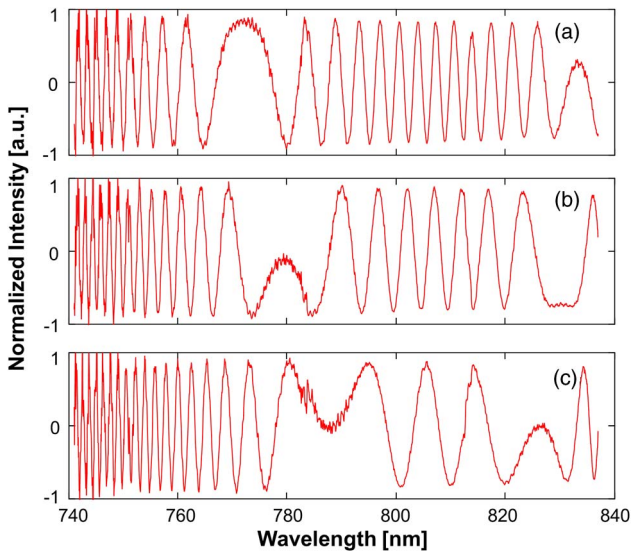


Fig. 2. Recorded normalized interferograms at (a) −400, at (b) −200, and at (c) 0 fs relative delays.

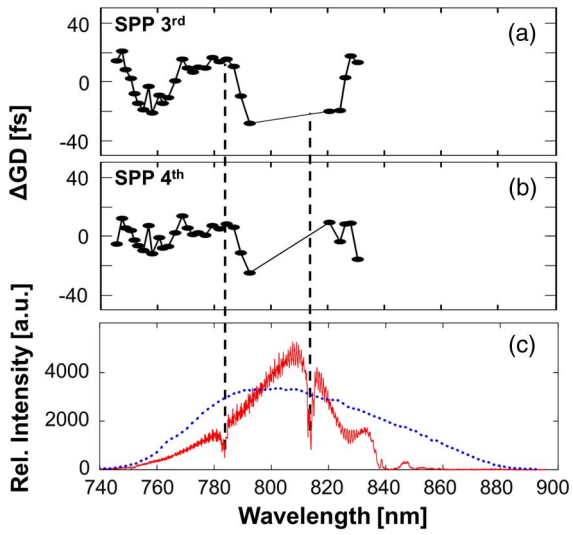


Fig. 3. Difference between the fitted (a) third and (b) fourth-order polynomial and the measured group delay curve obtained by the SPP method. (c) Spectrum of the sample pulse (red) and of the Ti:S laser (dotted blue). The spectral positions of the leaking modes are denoted with dashed lines.

the phase extraction was between −1700 and 240 fs. In the case of fourth-order polynomial fitting, the difference between the measured and the fitted curve is displayed in Fig. 5(a). By comparing it to the results from a fifth-order fitting, it can be clearly seen that the difference is much smaller in the case of fifth-order dispersion retrieval [Fig. 5(b)]. The retrieved spectral phase as a function of wavelength is shown in Fig. 6 in the case of fifth-order dispersion retrieval. According to the significant difference between the fitted and measured spectral phase, regardless of the order of the fitted polynomial (see Fig. 5), we concluded that this method is less applicable if higher order dispersion is of concern.

The 30 interferograms evaluated with the MM method were also evaluated by CFF method in the same delay range. The result from fitting a phase modulated cosine function with a fourth-order polynomial in its argument can be seen in Fig. 7(a). It can be concluded the fourth-order fit might not be sufficient as a misfit around the second SPP is clearly observable on the interferogram. By fitting a cosine function with a fifth-order polynomial in its argument a much better fit is achievable than in the former case [see Fig. 7(b)].

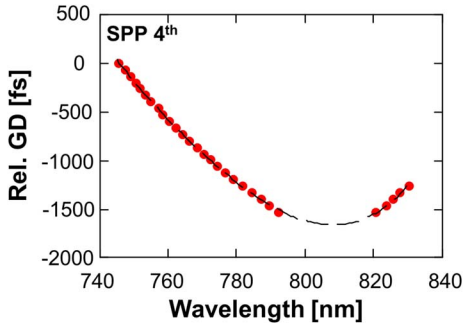


Fig. 4. Measured (red) and fitted (dashed black) relative group delay as a function of the wavelength obtained by the SPP method.

As mentioned before, the spectral transmission of the PBG fiber has resonances at 783 and 813 nm [see Fig. 3(c)], where the spectral phase function has sharp peaks. As there is no observable difference between the normalized interferogram and the fitted curve in the vicinity of these resonances, this method does not allow the measurement of such irregularities. Despite this limitation, we have come to the conclusion that the CFF method is applicable to measure higher order dispersion. We noticed that the fit was more sensitive to higher order terms if both SPPs fell into the evaluation range of the interferogram. Apparently, in our case the highest decisive term happen to be the fifth, as can be seen from fit (Fig. 4). This is a result also presumed from the previous evaluations.

Hereinafter, the results from the FT procedure are presented. Seventeen interferograms were recorded at larger time delays (from −5700 to −2100 and from 1200 to 5500 fs) in order to produce sufficiently dense fringes. The steps of the evaluation are shown in Fig. 8 below. The linear term was subtracted from the retrieved spectral phase in order to demonstrate the influence of the higher order dispersion terms, especially the TOD, the significance of which has been already demonstrated by the two SPPs appearing on the interferograms.

The sensitivity of the method to the higher order dispersion was tested by fitting a fourth and a fifth-order polynomial to the spectral phase curve. Figure 9 shows the phase difference between the measured and the fitted spectral phase function in the two cases. The sharp peaks of the spectral phase can be seen well in both cases, but the misfit is smaller in the case of the fifth-order fit. It can be

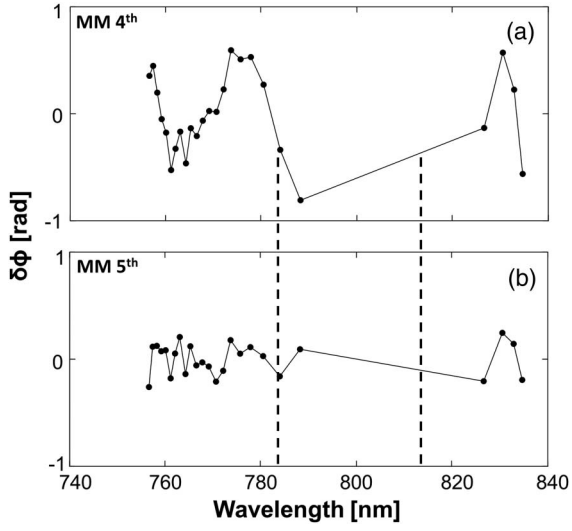


Fig. 5. Difference between the fitted (a) fourth and (b) fifth-order polynomial and the measured spectral phase curve obtained by the MM method. The spectral positions of the leaking modes are denoted with dashed lines.

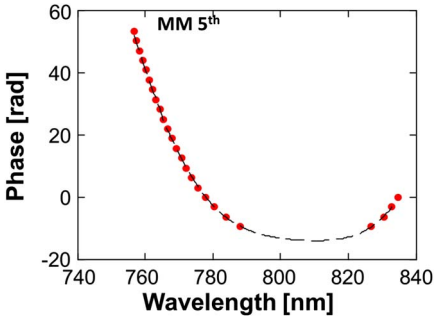


Fig. 6. Measured (red) and fitted (dashed black) spectral phase obtained by the MM method.

concluded that the FT method is very sensitive and accurate.

The applicability of the WFT method was also tested on the same 17 interferograms containing dense fringes. The windowed Fourier transform of a recorded spectral interferogram is displayed in Fig. 10. The most precise group delay versus frequency function was obtained when the width of the window function was $\Delta\Omega = 0.003$ PHz. 200 window functions with various central frequencies were used in order to cover the whole spectral range of the interferogram. The time duration of the interference terms obtained by applying a FT on the windowed interferograms was approximately 2 ps. The position of the peak of this signal in the time domain was measured with an accuracy of 10 fs.

Having the group delay obtain a third-order polynomial was fitted in order to determine the dispersion coefficients up to the fourth term. To retrieve the fifth-order dispersion, a fourth order polynomial was also used. As can be seen in Fig. 11, the fit is better in the case of the fourth order polynomial, as the difference between the fitted and the measured group delay curve oscillates around zero, of course, except in the vicinity of the leaking mode frequencies where it shows sharp peaks. Thus, it can be concluded that determining the dispersion coefficients up to the fifth order is necessary, as expected from the results of the

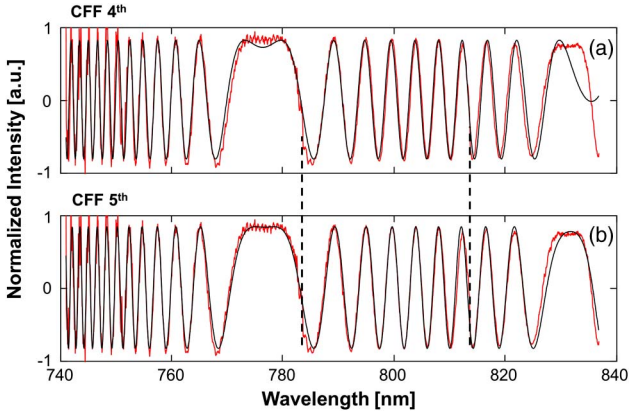


Fig. 7. Normalized spectral interferograms with the results of the CFF with (a) fourth and (b) fifth-order polynomial in its argument (red, measured data; black solid line, fitted curve). The spectral positions of the leaking modes are denoted with dashed lines.

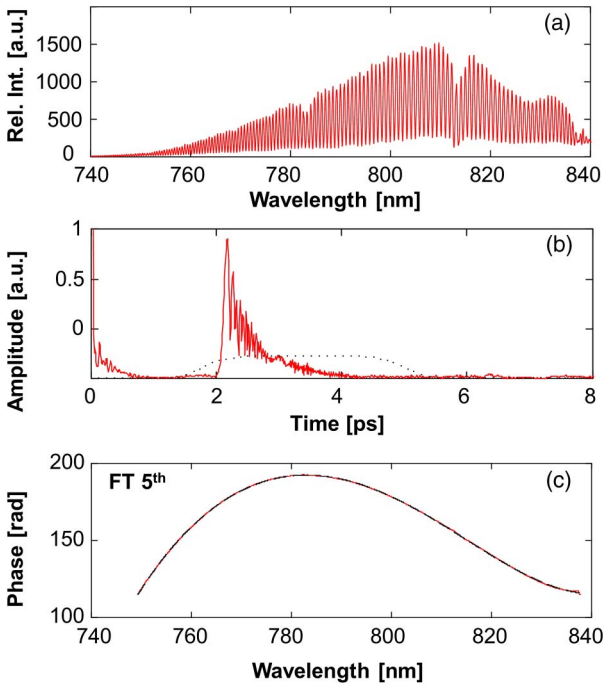


Fig. 8. (a) Recorded spectral interferogram, (b) the FT of the interferogram, and (c) the retrieved (red) and the fitted (dashed black) spectral phase obtained by the FT method without the linear phase term.

previous methods. Note that this method could also detect the phase jumps at the leaking mode frequencies regardless of the fitting order. However, this evaluation procedure proved to be a bit time-consuming.

The dispersion coefficients up to the fifth order retrieved with repetitive measurements by the five evaluation methods are presented in Table 1. It can be seen that the conventional FT method has the highest accuracy that could be due to the fact that it provides the spectral phase as a quasi-continuous function of the frequency and does not rely on polynomial fitting. The CFF evaluation also seems to have a high precision while the accuracy of the WFT method falls short of expectations. In this case of the latter method high spectral resolution was required in order to resolve the leaking mode frequencies. This

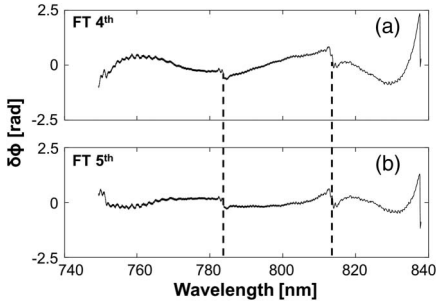


Fig. 9. Difference between the measured spectral phase obtained by the FT method and the fitted (a) fourth and (b) fifth-order polynomial. The spectral positions of the leaking modes are denoted with dashed lines.

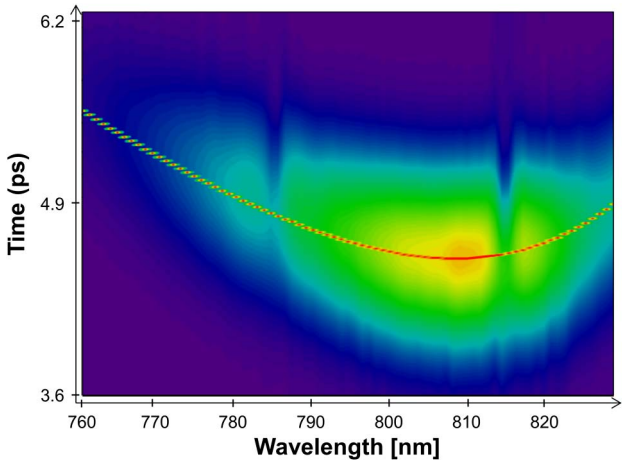


Fig. 10. Windowed FT of a spectral interferogram with the measured group delay curve obtained by the WFT method.

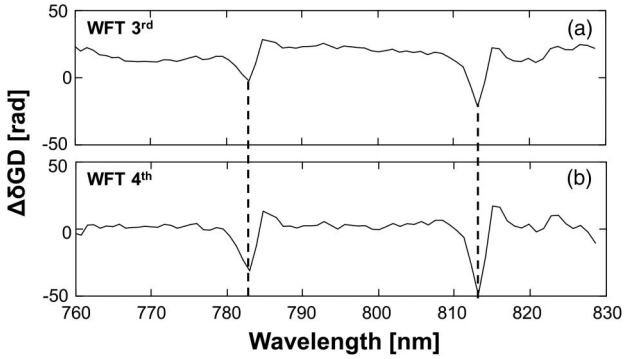


Fig. 11. Difference between the measured and the fitted (a) third and (b) fourth-order group delay curves obtained by the WFT method. The spectral positions of the leaking modes are denoted with dashed lines.

resulted in broadening of the FT of the windowed interferogram in time thus determination of the peaks of the fringes became less accurate. The accuracy of the SPP and the MM methods is also worse in comparison to the other methods.

By comparing the values of the retrieved GDD to the GDD of a conventional silica single-mode fiber of the same length, which is about one order of magnitude higher (~13360 $fs^2$ at 800 nm) it becomes obvious that the tested solid core PBG fiber has a reduced second-order dispersion due to the superimposed effect of anomalous waveguide dispersion [17]. At the expense of the reduced GDD, the higher order terms become significant. We compared the determined TOD values to the TOD values of the same silica single-mode fiber and found that it was about one magnitude lower (~10152 $fs^3$ at 800 nm) in the case of the silica fiber. This observation is also confirmed by the fact that two SPPs appear on the interferograms.

## 5. Summary

A comparative study of five evaluation methods for measuring the chromatic dispersion of a solid-core short-length PBG fiber was presented. Our technique, which is based on spectral interferometry employing a high resolution spectrometer and a Ti:sapphire oscillator as a light source, utilizes a Mach–Zehnder interferometer with a fiber under study in its one arm.

It was demonstrated that the tested PBG fiber sample has relatively low second-order dispersion compared to conventional single mode fibers. However, in case of this specific design, the higher order terms become larger than that of conventional silica fibers due to the superimposed effect waveguide dispersion and leaking modes appearing within the bandgap.

In order to calculate the refractive index profile of the realized fiber, measuring the amplitude spectrum and a precise retrieval of the spectral phase is essential. As demonstrated, the traditional FT method met these requirements as it provided the dispersion coefficients up to the fifth order with the highest accuracy. The CFF method also proved to be very sensitive to the presence of higher order dispersion terms. Only the evaluations based on FT could accurately detect the phase jumps in the vicinity of the leaking modes in the spectrum of the fiber.

We thank Mr. Borut Lenardic (OptaCore, Slovenia) for providing the fiber samples and related informations for our dispersion measurements and numerical simulations. This research was partially supported by the European Union and the State of Hungary, co-financed by the European Social Fund in the framework of TÁMOP-4.2.4.A/2-11/1-2012-0001 "National Excellence Program." The project was partially funded by "TÁMOP-4.2.2.A-11/1/KONV-2012-0060—Impulse lasers for use in materials science and biophotonics," which is supported by the European Union and co-financed by the European Social Fund. This work was supported by the National Development Agency under grant TECH-09-A2-2009-0134 and also by OTKA contract no. 76404.

**Table 1. Dispersion Coefficients of a 37 cm Long PBG Fiber at 800 nm Obtained by the Five Evaluation Methods**

| | SPP | MM | CFF | FT | WFT |
|---|---|---|---|---|---|
| GDD [$fs^2$] | 2116 ± 260 | 1980 ± 192 | 2086 ± 45 | 2076 ± 30 | 2985 ± 220 |
| TOD [$10^5$ $fs^3$] | 1.324 ± 0.045 | 1.17 ± 0.19 | 1.272 ± 0.031 | 1.244 ± 0.023 | 1.273 ± 0.035 |
| FOD [$10^6$ $fs^4$] | −1.94 ± 0.34 | −1.27 ± 0.31 | −1.94 ± 0.34 | −1.893 ± 0.060 | −1.82 ± 0.40 |
| QOD [$10^7$ $fs^5$] | 1.95 ± 0.53 | 1.06 ± 0.52 | 2.11 ± 0.13 | 2.21 ± 0.13 | 2.4 ± 1.4 |

## References


1. P. Yeh, A. Yariv, and E. Marom, "Theory of Bragg fiber," J. Opt. Soc. Am. **68**, 1196–1201 (1978).
2. J. Fekete, Z. Várallyay, and R. Szipőcs, "Design of high-bandwidth one- and two dimensional photonic bandgap dielectric structures at grazing incidence of light," Appl. Opt. **47**, 5330–5336 (2008).
3. J. C. Knight, T. A. Birks, P. St. J. Russell, and D. M. Atkin, "All-silica single-mode optical fiber with photonic crystal cladding," Opt. Lett. **21**, 1547–1549 (1996).
4. J. Broeng, D. Mogilevstev, S. E. Barkou, and A. Bjarklev, "Photonic crystal fibers: a new class of optical waveguides," Opt. Fiber Technol. **5**, 305–330 (1999).
5. A. Ferrando, E. Silvestre, J. J. Miret, and P. Andrés, "Nearly zero ultraflattened dispersion in photonic crystal fibers," Opt. Lett. **25**, 790–792 (2000).
6. T. P. White, R. C. McPhedran, C. Martijin de Sterke, N. M. Litchinister, and B. J. Eggleton, "Resonance and scattering in microstructured fibers," Opt. Lett. **27**, 1977–1979 (2002).
7. P. St. J. Russell, "Photonic-crystal fibers," J. Lightwave Technol. **24**, 4729–4749 (2006).
8. Q. Fang, Z. Wang, L. Jin, J. Liu, Y. Yue, Y. Liu, G. Kai, S. Yuan, and X. Dong, "Dispersion design of all-solid photonic bandgap fiber," J. Opt. Soc. Am. B **24**, 2899–2905 (2007).
9. Z. Várallyay, K. Saitoh, J. Fekete, K. Kakihara, M. Koshiba, and R. Szipőcs, "Reversed dispersion slope photonic bandgap fibers for broadband dispersion control in femtosecond fiber lasers," Opt. Express **16**, 15603–15615 (2008).
10. Z. Várallyay, K. Saitoh, Á. Szabó, and R. Szipőcs, "Photonic bandgap fibers with resonant structures for tailoring the dispersion," Opt. Express **17**, 11869–11883 (2009).
11. L. G. Cohen, "Comparison of single-mode fiber dispersion measurement techniques," J. Lightwave Technol. **3**, 958–966 (1985).
12. M. A. Galle, W. Mohammed, L. Qian, and P. W. E. Smith, "Single-arm three-wave interferometer for measuring dispersion of short lengths of fiber," Opt. Express **15**, 16896–16908 (2007).
13. C. Sáinz, P. Jourdain, R. Escalona, and J. Calatroni, "Real-time interferometric measurements of dispersion curves," Opt. Commun. **111**, 632–641 (1994).
14. H.-T. Shang, "Chromatic dispersion measurement by white-light interferometry on metre-length single-mode optical fibres," Electron. Lett. **17**, 603–605 (1981).
15. F. Koch, S. V. Chernikov, and J. R. Taylor, "Dispersion measurement in optical fibres over the entire spectral range from 1.1 μm to 1.7 μm," Opt. Commun. **175**, 209–213 (2000).
16. P. Hlubina, M. Szpulak, D. Ciprian, T. Martynkien, and W. Urbanczyk, "Measurement of the group dispersion of the fundamental mode of holey fiber by white-light spectral interferometry," Opt. Express **15**, 11073–11081 (2007).
17. J. Jasapara, T. H. Her, R. Bise, R. Windeler, and D. J. DiGiovanni, "Group-velocity dispersion measurements in a photonic bandgap fiber," J. Opt. Soc. Am. B **20**, 1611–1615 (2003).
18. J. Y. Lee and D. Y. Kim, "Versatile chromatic dispersion measurement of a single mode fiber using spectral white light interferometry," Opt. Express **14**, 11608–11615 (2006).
19. L. Zong, F. Luo, S. Cui, and X. Cao, "Rapid and accurate chromatic dispersion measurement of fiber using asymmetric Sagnac interferometer," Opt. Lett. **36**, 660–662 (2011).
20. P. Hlubina, M. Kadulová, and D. Ciprian, "Spectral interferometry-based chromatic dispersion measurement of fibre including the zero-dispersion wavelength," J. Eur. Opt. Soc. Rapid Pub. **7**, 12017-1–12017-5 (2012).
21. Q. Ye, Ch. Xu, X. Liu, W. H. Knox, M. F. Yan, R. S. Windeler, and B. Eggleton, "Dispersion measurement of tapered air–silica microstructure fiber by white-light interferometry," Appl. Opt. **41**, 4467–4470 (2002).
22. T. M. Kardas and C. Radzewicz, "Broadband near-infrared fibers dispersion measurement using white light interferometry," Opt. Commun. **282**, 4361–4365 (2009).
23. L. Lepetit, G. Chériaux, and M. Joffre, "Linear techniques of phase measurement by femtosecond spectral interferometry for applications in spectroscopy," J. Opt. Soc. Am. B **12**, 2467–2474 (1995).
24. S. Diddams and J.-C. Diels, "Dispersion measurements with white-light interferometry," J. Opt. Soc. Am. B **13**, 1120–1129 (1996).
25. Ch. Dorrer, "Influence of the calibration of the detector on spectral interferometry," J. Opt. Soc. Am. B **16**, 1160–1168 (1999).
26. Ch. Dorrer, N. Belabas, J. P. Likforman, and M. Joffre, "Spectral resolution and sampling issues in Fourier-transform spectral interferometry," J. Opt. Soc. Am. B **17**, 1795–1802 (2000).
27. G. Genty and H. Ludvigsen, "Measurement of anomalous dispersion in microstructured fibers using spectral modulation," Opt. Express **12**, 929–934 (2004).
28. S. K. Debnath, M. P. Kothiyal, and S.-W. Kim, "Evaluation of spectral phase in spectrally resolved white-light interferometry: comparative study of single-frame techniques," Opt. Laser Eng. **47**, 1125–1130 (2009).
29. N. K. Berger, B. Levit, and B. Fischer, "Measurement of fiber chromatic dispersion using spectral interferometry with modulation of dispersed laser pulses," Opt. Commun. **283**, 3953–3956 (2010).
30. L. Huang, Q. Kemao, B. Pan, and A. K. Asundi, "Comparison of Fourier transform, windowed Fourier transform, and wavelet transform methods for phase extraction from a single fringe pattern in fringe projection profilometry," Opt. Laser Eng. **48**, 141–148 (2010).
31. P. Hlubina, J. Luňáček, D. Ciprian, and R. Chlebus, "Windowed Fourier transform applied in the wavelength domain to process the spectral interference signals," Opt. Commun. **281**, 2349–2354 (2008).
32. P. Hlubina, J. Luňáček, and D. Ciprian, "Spectral interferometry and reflectometry used for characterization of a multilayer mirror," Opt. Lett. **34**, 1564–1566 (2009).
33. Z. Luo, S. Zhang, W. Shen, C. Xia, Q. Ma, X. Liu, and Y. Zhang, "Group delay dispersion measurement of a dispersive mirror by spectral interferometry: comparison of different signal processing algorithms," Appl. Opt. **50**, C239–C245 (2011).
34. A. Börzsönyi, A. P. Kovács, M. Görbe, and K. Osvay, "Advances and limitations of phase dispersion measurement by spectrally and spatially resolved interferometry," Opt. Commun. **281**, 3051–3061 (2008).
35. S. Février, R. Jamier, J.-M. Blondy, S. L. Semjonov, M. E. Likhachev, M. M. Bubnov, E. M. Dianov, V. F. Khopin, M. Y. Salganskii, and A. N. Guryanov, "Low-loss singlemode large mode area all-silica photonic bandgap fiber," Opt. Express **14**, 562–569 (2006).
36. K. Mecseki and A. P. Kovács, "Monitoring of residual higher-order dispersion of pulse compression by spectral interferometry," AIP Conf. Proc. **1228**, 251–256 (2010).